

## Article

# Geochemistry and Petrology of Reservoir and Cap Rocks in Zar-3 Pilot CO<sub>2</sub> Storage Complex, SE Czechia

Juraj Francu <sup>1,\*</sup> , Daniela Ocásková <sup>1</sup>, Petr Pařízek <sup>1</sup>, Jakub Vácha <sup>1</sup>, Miroslav Pereszlenyi <sup>1</sup>, Petr Jirman <sup>1</sup> , Vladimír Opletal <sup>2</sup> and Monika Ličbinská <sup>3</sup> 

<sup>1</sup> Czech Geological Survey, Leitnerova 22, 60200 Brno, Czech Republic; daniela.ocaskova@geology.cz (D.O.); jakub.vacha@geology.cz (J.V.); pereszlenyi@pcg.sk (M.P.); petr.jirman@geology.cz (P.J.)

<sup>2</sup> MND a.s., Úprkova 807/6, 69501 Hodonín, Czech Republic; opletal@mnd.cz

<sup>3</sup> Department of Geological Engineering, VŠB—Technical University Ostrava, 17. Listopadu 15, 70800 Ostrava-Poruba, Czech Republic; monika.licbinska@vsb.cz

\* Correspondence: juraj.francu@geology.cz

**Abstract:** The planned pilot CO<sub>2</sub> storage Zar-3 is an oil field with a gas cap in the final production stage in the SE Czech Republic. It is composed of a dolomite Jurassic reservoir sealed by three different formations that differ significantly in lithology. Previous studies left open questions on the nature of pore space and connectivity and the quality of the seal in the future CO<sub>2</sub> storage complex. Microscopic petrography of the reservoir suggests dolomitisation in shallow water followed by karstification and brecciation with fracture-correct-dominated porosity. The seal horizons have porosity limited to the micro- and nanoscales. The oil consists of significantly biodegraded black oil of Jurassic origin mixed with less biodegraded gasoline-range hydrocarbons. Biomarkers in the caprock bitumens trapped in nanopores show a genetic relationship to the reservoir oil. Gas in the not yet fully depleted gas cap of the field is of thermogenic origin with no contribution of microbial methane. The formation water has total dissolved solids typical of isolated brines not diluted by infiltrated fresh water. The geochemical characteristics of the storage system together with the fact that the initial oil column is about 105 m tall with another 150 m of gas cap suggest that the seals are efficient and the Zar-3 future storage complex is tight and safe.

**Keywords:** CCS; geochemistry; petrography; reservoir rock; cap rock; porosity; formation water; Zar-3; pilot CO<sub>2</sub>



**Citation:** Francu, J.; Ocásková, D.; Pařízek, P.; Vácha, J.; Pereszlenyi, M.; Jirman, P.; Opletal, V.; Ličbinská, M. Geochemistry and Petrology of Reservoir and Cap Rocks in Zar-3 Pilot CO<sub>2</sub> Storage Complex, SE Czechia. *Geosciences* **2024**, *14*, 119. <https://doi.org/10.3390/geosciences14050119>

Academic Editors: Salvatore Critelli and Jesus Martinez-Frias

Received: 5 March 2024

Revised: 11 April 2024

Accepted: 20 April 2024

Published: 28 April 2024



**Copyright:** © 2024 by the authors. Licensee MDPI, Basel, Switzerland. This article is an open access article distributed under the terms and conditions of the Creative Commons Attribution (CC BY) license (<https://creativecommons.org/licenses/by/4.0/>).

## 1. Introduction

The main purpose of this paper is to provide knowledge about the composition and properties of the reservoirs, caprocks and fluids of the planned Zar-3 CO<sub>2</sub> storage complex, which is an oil and gas field in the final phase of production that will be depleted in the near future. The motivation is to provide necessary geochemical data for predictions of how the reservoir and seal rocks will react to the injection of supercritical carbon dioxide. In the reservoir, the most important questions are whether the porosity and permeability will increase or decrease after the injection of CO<sub>2</sub> and how far from the injection point mineral dissolution and neof ormations will occur. In caprock horizons, the principal question is the current seal efficiency and its potential change after the injection of CO<sub>2</sub>. For those purposes, the detailed chemical and mineral composition of reservoirs and caprocks were studied using different complementary methods together with petrology and pore space geometry. Previous studies [1–4] outlined the geological setting in the SE Bohemian Massif below the West Carpathians but did not include the necessary petrological and geochemical details. The results of this paper are intended to be used to better constrain geomechanical investigations, dynamic modelling and risk assessment of the Zar-3 storage site. The results serve as a basis for predictive estimation of how the rocks will accept or resist carbon dioxide storage.

## 2. Geological Setting

The Zar-3 area of interest and broader neighbourhood belong to the most important petroleum systems in SE Czechia [1–4]. The Zar-3 planned pilot CO<sub>2</sub> storage site (Figure 1) consists of the following units from top downwards (Figure 2):

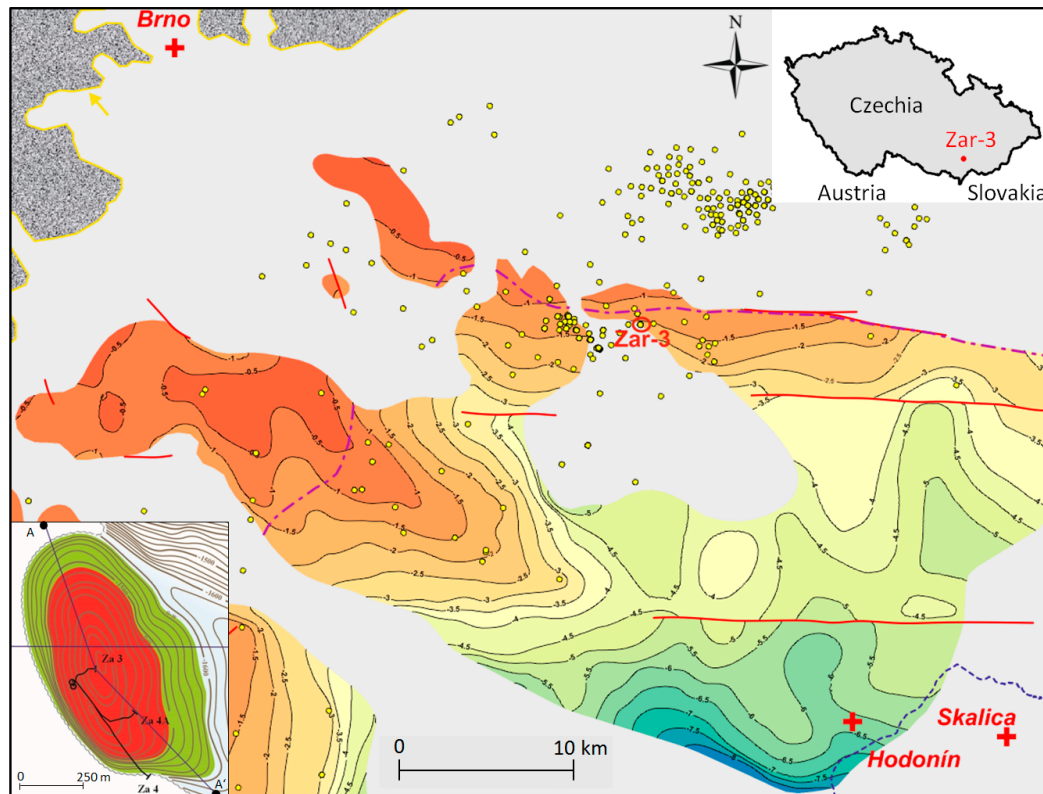


**Figure 1.** Location of the planned Zar-3 storage site (red circle and lower left insert, where red: gas, green: oil) and adjacent region with buried top of Jurassic erosional relicts of the SE Bohemian Massif, contour lines are in km below sea level. Yellow dots show >900 m deep boreholes, purple dash-and-dot line outlines the NW erosional margin of the Mikulov Fm. (seal 1 in Zar-3).

### Overburden:

- Overthrust Ždánice unit with Ždánice-Hustopeče, Menilite and Němčice Fms. (caprock 3—shales);
- Autochthonous Middle Paleogene—Nesvačilka Fm. (caprock 2—sandy and shaly siltstone);
- Upper Jurassic—Mikulov Fm. (caprock 1—marl).

### Reservoir:

- Upper Jurassic—Vranovice Fm. (main reservoir—dolomite);
- Middle Jurassic—Nikolčice Fm. (additional reservoir underlying the Vranovice Fm.—siliceous sandstone);
- Middle Jurassic—Gresten Fm. (additional reservoir—quartz sandstone) does not occur in Zar-3 but nearby.

### Underburden:

- Possibly Upper Carboniferous—Ostrava Fm. (sandstone with coal seams);
- Lower Carboniferous—Myslejovice Fm. (sandstone/shale turbidites);
- Middle to Upper Devonian—Old Red Fm. (sandstone and cemented conglomerate); Macocha and Líšeň Fms. (carbonates);
- Crystalline basement.

Paleozoic strata were significantly eroded prior to the Tethys ocean opening and the evolution of passive margin basins in the Middle and Upper Jurassic [1,4]. In the Cretaceous and Early Paleogene, two deep submarine canyons were incised into the Jurassic and filled by siliciclastic sediments in the Middle Paleogene [2–4]. In the Early-Middle Miocene, the Ždánice unit of the West Carpathian fold-and-thrust belt was emplaced on the SE margin of the Bohemian Massif, burying the source and reservoir rocks, and the petroleum system formed [3,4]. In Zar-3, the initial oil column was 105 m; currently, it is 20 m. The initial gas cap was 150 m thick; now, it is 195 m. While the initial reservoir pressure was 17.6 MPa, currently it is 12.5 MPa at a depth of 1760 m, where the temperature is about 53 °C.

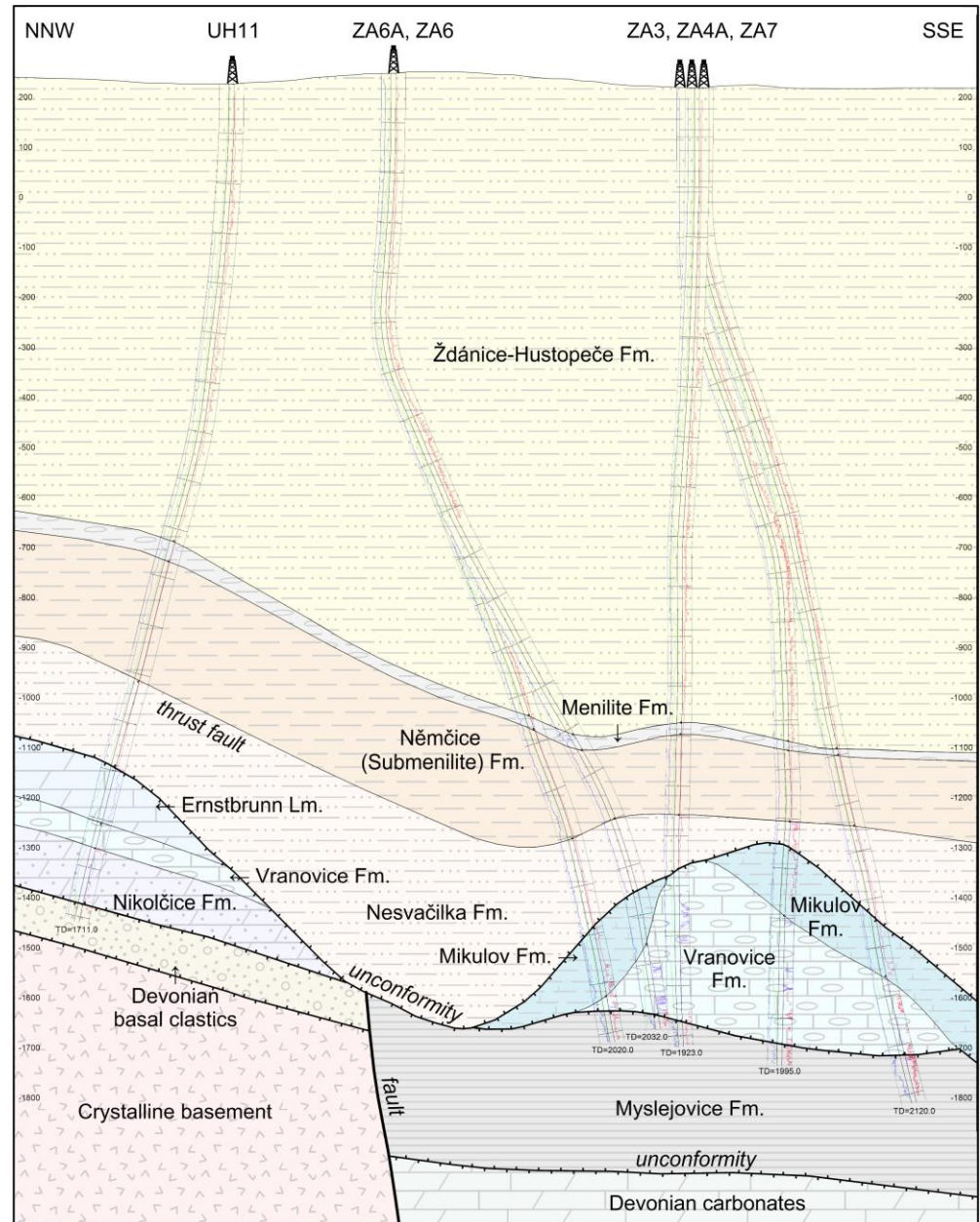


**Figure 2.** NNW-SSE section through the Zar-3 storage site with reservoir—Vranovice Fm., top seals—Mikulov Fm., Nesvačilka Fm., Němčice Fm. above the thrust plane of the Ždánice unit and bottom seal—Myslejovice Fm. For location of the AA' section, see lower left insert in Figure 1.

### 3. Samples

Firstly, 68 core samples were provided by MND from the core repository together with the MudLogs and well logs, which made it possible to estimate the depth interval represented by the core samples. In addition, 121 cuttings samples were provided by MND from the ZA3 well, which cover the measured depth interval of 1200–1923 m (TVDSS 978–1699 m). The positions of the core and cuttings samples are shown in Figure 3. A sample list of the reservoirs and caprocks is in Supplementary Table S1 with the true vertical sub-sea depth (TVDSS m) of the samples, lithostratigraphy and further details.

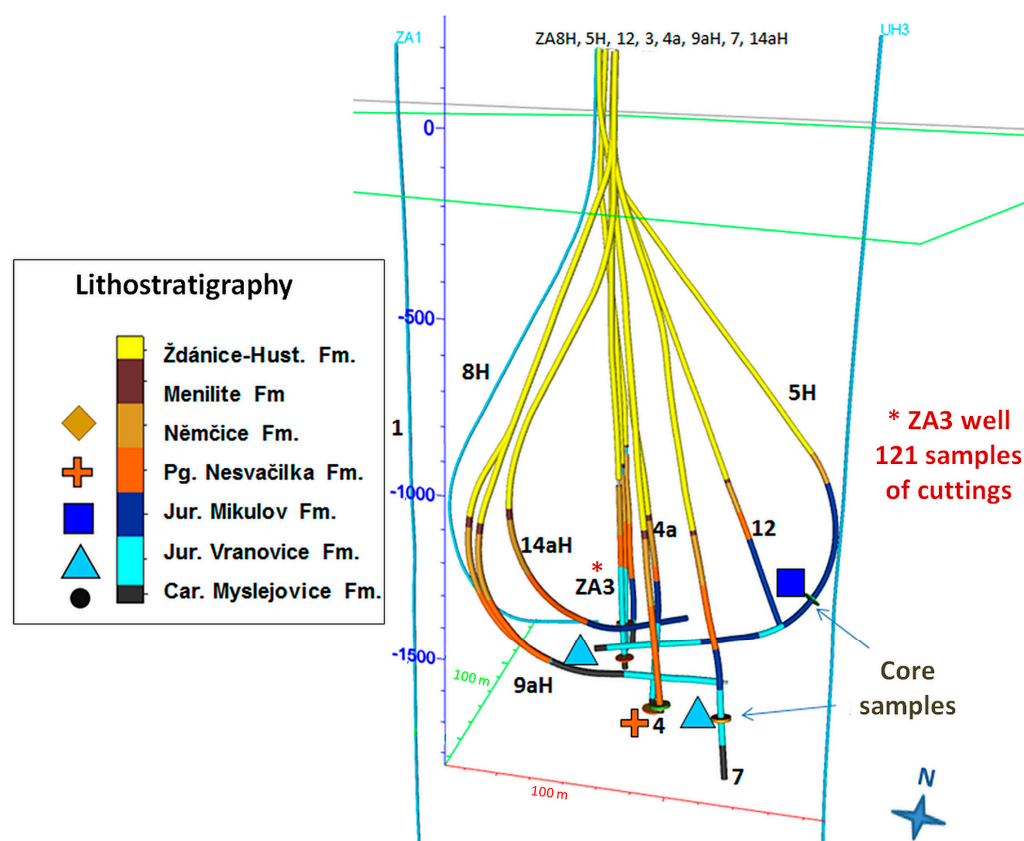


**Figure 3.** Position of 68 cores (different wells) and 121 cuttings samples (ZA3 profile) for geochemical analyses. Žarošice (ZA) well numbers are shown next to each well trajectory. Core samples are shown as disks with symbol and color for lithostratigraphy.

### 4. Experimental Methods

The elemental composition of total organic carbon (TOC), total inorganic carbon (TIC) and total sulphur (TS) were analysed using an ELTRA<sup>®</sup> 2000 instrument with three infrared detectors. TIC was measured using a phosphoric acid treatment and TOC and TS by oxidation in oxygen flow at 1420 °C after the removal of carbonates by HCl at 40 °C. TIC was recalculated stoichiometrically to calcite or dolomite content based on XRD. Rock-Eval 6 pyrolysis was used on selected samples providing free and pyrolytic hydrocarbon in rock. The mineral composition was analysed using the powder X-ray diffraction method with CuK $\alpha$  irradiation. X-ray fluorescence (XRF) was used for bulk chemical composition.

Selected pieces of rocks were divided into slabs, which were vacuum impregnated with blue epoxy resin, and polished thin sections were prepared. Mineralogy, pore space and pore throats were described using optical microscopy. Fluorescence light microscopy made it possible to indicate the presence of hydrocarbon micro-fluid inclusions. Optical microscopy was made in non-polarised light (NPL) plane polarised light (PPL), cross-polarised light (XPL) and fluorescent light using a Leitz Orthoplan<sup>®</sup> (Germany) microscope MPV-II with the Ploemopak fluorescence module, which was used with a blue-violet

excitation light of 400 nm wavelength, dichromatic mirror of 510 nm to remove the low wavelength light, and finally a 510 nm barrier filter to remove the excitation light from the outgoing light. The microscope was equipped with a XBO 450 xenon lamp. Thin sections were further scanned by an optical NIKON® scanner and 2 × 3 cm sample pictures were produced.

Soluble organic matter was extracted from rocks using a Dionex® accelerated extractor by a DCM–methanol mixture (97 + 3) and the solution volume was reduced by Turbovap. Elemental sulphur was removed by activated copper. Saturated (SAT), aromatic (ARO) and polar (NSO) fractions were separated on a silica column. SAT and ARO fractions were analysed by gas chromatography–mass spectrometry (Agilent 7890A and 5973N MSD). Mass chromatograms were evaluated as peak areas and molecular biomarkers ratios calculated using three NIGOGA standards or rather reference samples purchased from the Norwegian Petroleum Directorate (NIGOGA 2000).

The isotopic composition of  $\delta^{13}\text{C}(\text{CH}_4)$  was measured using the “Trace GC, IsoLink” combustion unit and Delta V isotope mass spectrometer (Thermo Fisher Scientific®). The T iso2, L iso1 of Isometric Instruments (Victoria, BC, Canada) were used in ConFlow 4 as a reference methane mixture for calibration. Carbon and hydrogen isotope ratios are reported in the usual delta notation ( $\delta^{13}\text{C}$ ,  $\delta\text{D}$  meaning  $\delta^2\text{H}$ ) relative to Vienna-Pee Dee Belemnite (VPDB) and Vienna-Standard Mean Ocean Water (VSMOW), respectively.

## 5. Results

A total of 68 cores and 121 cuttings samples were analysed for total inorganic carbon (TIC), total organic carbon (TOC) and total sulphur (TS); the results are in Supplementary Tables S1 and S2. Geochemical proxy parameters were used to evaluate the properties of sedimentary strata and the petroleum systems following, e.g., [5–8] in Zar-3. The quantitative results of the measured parameters are in the following Supplemental Tables S1 and S2—Carbonates, TOC, TS and cation exchange capacity (CEC) in the ZA3 well cuttings and core samples from different wells; Table S3—Rock-Eval pyrolysis of the ZA3 cuttings; Table S4—mineral composition groups based on XRD; Table S5—thermal maturity of rocks and oils; Table S6—gas chemical and isotopic composition; Table S7—formation water chemistry in the reservoirs and permeable intervals of the caprocks. The results are discussed below with respect to other methods, such as MudLog data, with the aim of understanding whether the chemical composition was made during deposition, how much was altered during diagenesis to catagenesis, and how many migration events occurred until present. The conclusions are formulated as a starting point for predictions of changes in the system after future  $\text{CO}_2$  storage, which will be discussed in a follow-up paper.

## 6. Discussion

The results of the current study discussed below complement the previously published data dealing with the broader geological neighbourhood and petroleum systems, e.g., [2,9–11]. In addition, the unpublished archival MND and CGS data are used related to Zar-3.

### 6.1. Rock Type Based on TOC, TIC, TS and Rock-Eval Pyrolysis

The reservoirs and caprocks of the Zar-3 storage site differ among themselves in carbonate mineral content and total sulphur and form geochemical groups (Figures 4 and 5). The carbonate content in rocks was recalculated from TIC to dolomite for samples of the Vranovice Fm. and to calcite using chemical composition and mineralogy by XRD.

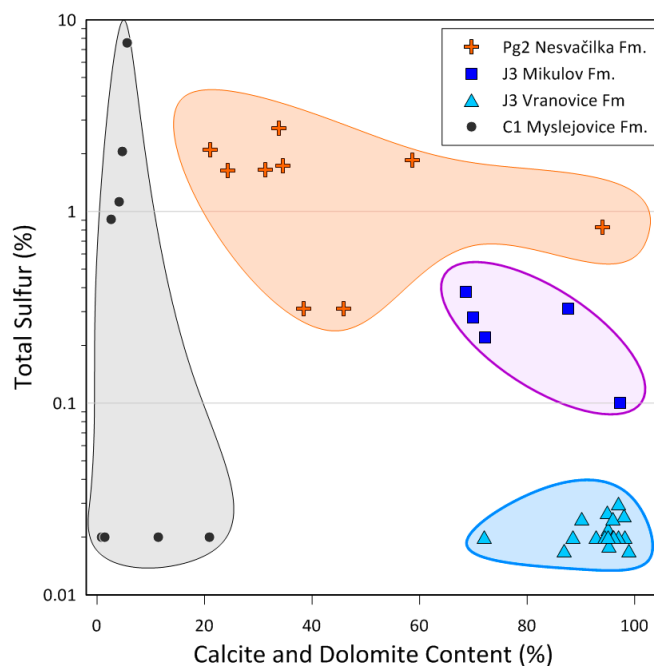


**Figure 4.** Total sulphur content versus carbonate mineral (calcite and dolomite) content in rocks in Zar-3 storage site calculated from total inorganic carbon (TIC) with respect to XRD mineralogy. Legend shows stratigraphy: Pg2—Middle Paleogene, J3—Upper Jurassic and C1—Lower Carboniferous together with the lithostratigraphic names of the formations.

While the dolomites of the Vranovice Fm. are very rich in inorganic carbon, they are lean in sulphur. Marls of the Mikulov Fm. show similar carbonate but elevated sulphur content. Nesvačilka Fm. contains a broad range of carbonate cements and high amount of sulphur, mostly as pyrite. Lower Carboniferous Myslejovice Fm. is very lean in carbonates and has a broad range of sulphur content, mostly as pyrite.

The geochemical profiles in Figures 5 and 6 based on carbon and sulphur elemental composition and Rock-Eval pyrolysis show the following trends in rock properties. The overthrust Ždánice-Hustopeče Fm. is composed of sandy siliciclastic sediments low in carbonates, intermediate in organic carbon, low in sulphur, low in hydrogen index (HI) and not very rich in expandable clays indicated by low CEC.

Menilite Fm. is exceptional with an elevated content of carbonate minerals in marls of the Dynów Mb., high organic carbon, very high sulphur and the highest HI, indicating high oil-prone source potential due to high algae input and anoxic depositional conditions. Similar observations in other wells in adjacent areas were mentioned earlier by [10–12]. Němčice formation was deposited in open marine (oceanic) conditions, with a low amount of carbonates and rather low TOC but sulphur as high as that in the upper part of the Menilite Fm. The expandable clay content based on CEC reaches the highest values of the entire profile and makes this unit probably the most efficient seal (caprock 3). The thermal maturity of the entire Ždánice overthrust unit is low and did not reach the beginning of the oil window.

The Nesvačilka Fm. (caprock 2) of Eocene age has higher calcareous cement component, very high TOC and HI typical of redeposited coaly particles with the contribution of marine kerogen type II. At much greater depths, this unit is a gas-prone source rock as mentioned earlier by [4,9]. No striking change in low thermal maturity ( $T_{max}$  in Figure 6) is observed at the overthrust/Nesvačilka Fm. (Paleogene) transition. This means that the uplift of the Ždánice unit and erosion of its upper part manifested as a diagenetic reversal in  $T_{max}$  were as extensive as has been observed in other parts of the Carpathian Flysch Belt, e.g., [1,9]. Free hydrocarbons (S1) reach notably high values (Figure 6) in this formation,

interpreted as oil impregnations of the siltstone dominated rock, which survived even washing the drilling mud away from the collected cuttings.

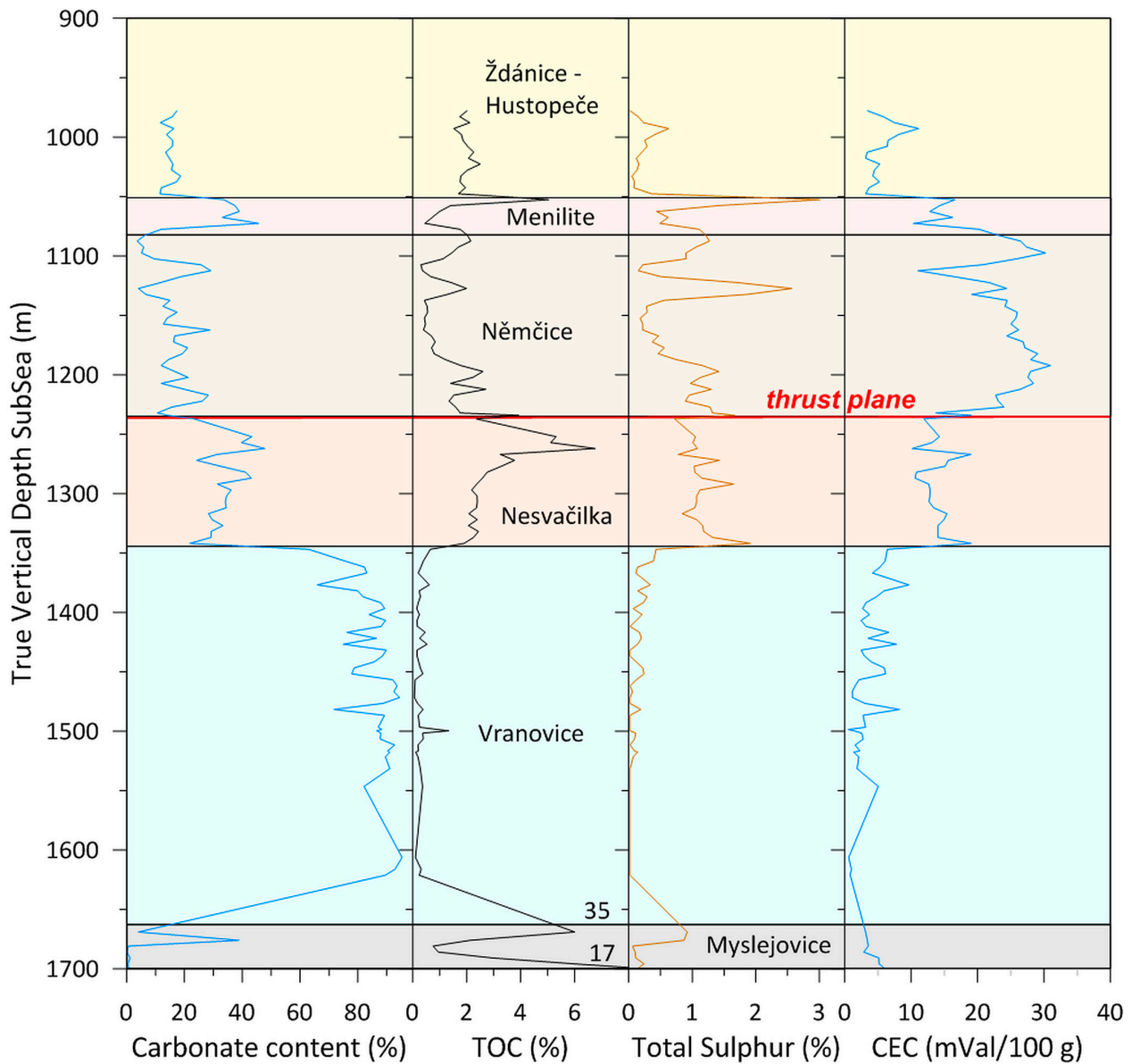


**Figure 5.** Carbonate content, total organic carbon (TOC), total sulphur (TS) and cation exchange capacity (CEC) with respect to true vertical depth (TVD SS) in drilling cuttings in the ZA3 well.

The Mikulov Fm. (caprock 1) was not encountered by the ZA3 well. The core samples from other wells in the Zar-3 area and in broader neighbourhood [13,14] provide TOC of 0.37–2.24%<sub>m</sub>, CaCO<sub>3</sub> of 34–77%<sub>m</sub>, S1 of 0.01–2.88 mg g<sup>-1</sup>, S2 of 1.28–9.10 mg g<sup>-1</sup>, and HI of 58–551 mg g<sup>-1</sup> TOC. The Mikulov Fm. is considered the principal source rock in the SE Bohemian Massif below the Flysch Belt and the Vienna Basin [4,9,15].

The main reservoirs consist of the Vranovice Fm. and underlying Nikolčice Fm. built by dolomites with 4–5 clay enriched horizons in the upper part (Figures 5 and 6). The formation is lean in sedimentary organic carbon and has low source potential (S1 + S2). Elevated hydrogen index and visual kerogen occur in the lower part. Our interpretation is that the low S1 in this reservoir interval is due to lower retention of hydrocarbons by dolomite and loss of free hydrocarbons during washing away the drilling mud from the cuttings samples. Macroscopically, the cores in this interval have brown coatings and smell of oil and the MudLogs show strong luminescence.

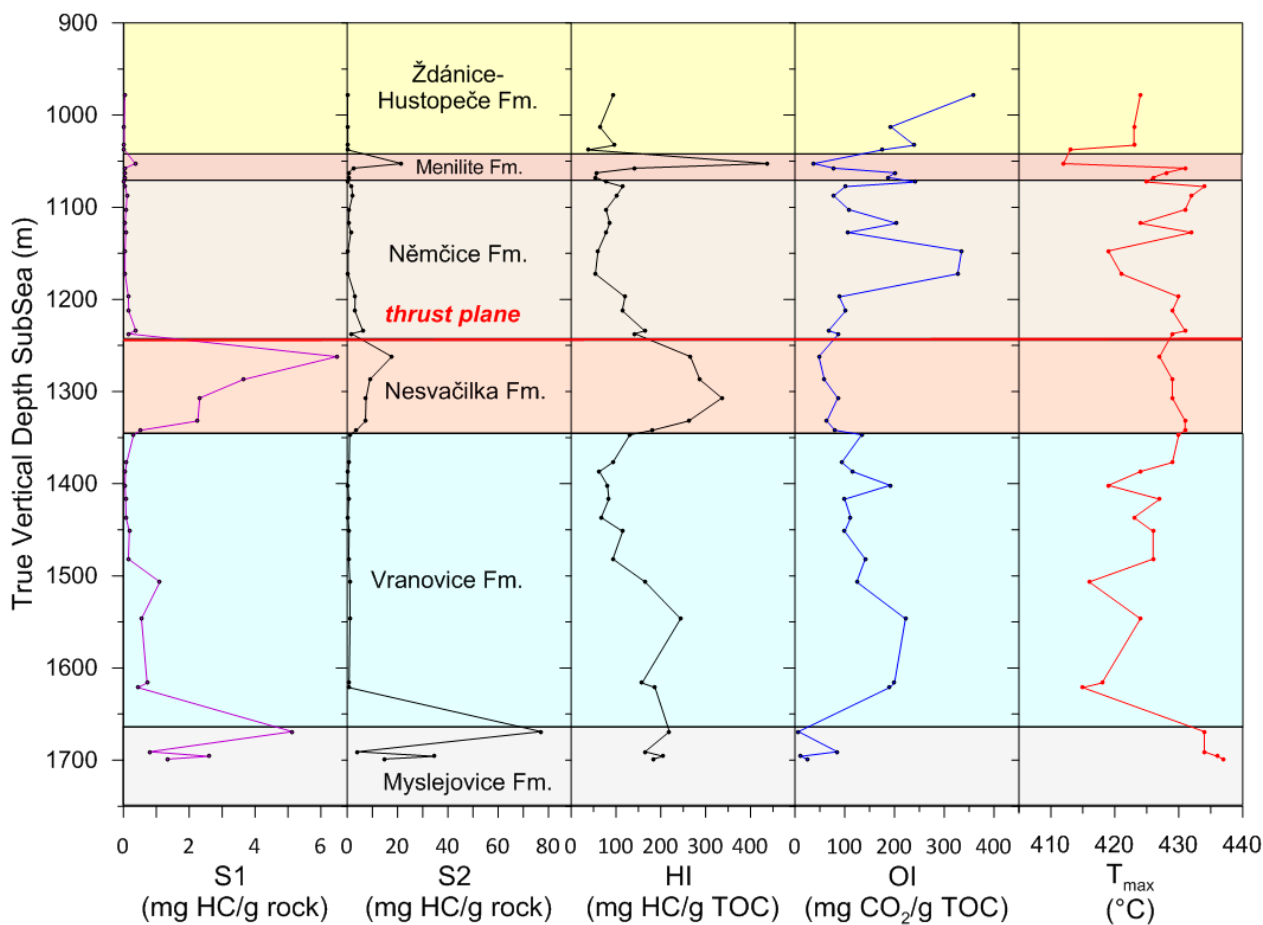


**Figure 6.** Free hydrocarbons (S1), pyrolytic hydrocarbons (S2), hydrogen index (HI), oxygen index (OI) and  $T_{\max}$  of kerogen with respect to true vertical depth (TVD SS) in cuttings from the ZA3 well profile.

The underlying Myslejšovice Fm. of Carboniferous age (bottom seal 4) has (with one exception) very low carbonate content in silty-shaly sandstones of deep water turbidites. Re-deposited coaly fragments make the TOC anomalously elevated in some of the Myslejšovice samples. HI indicates typical humic type III kerogen. Thermal maturity corresponding to the oil window is higher than that in the above part of the profile. This is interpreted as evidence of deeper burial and subsequent erosion of the upper part of Carboniferous strata prior to the Jurassic, as was observed earlier in the broader region [9,16]. This may be the reason why, due to increased catagenetic cementation, the porosity and permeability of the Myslejšovice Fm. are lower than those in the above strata.

### 6.2. Mineral Composition

Mineral composition was evaluated based on XRD, elemental composition, chemistry by XRF and microscopy. The data are in Supplementary Table S3. Selected samples representing the caprocks and reservoirs were also characterised by the wet chemistry method. The data show that the iron content in dolomites is low, i.e., that the iron-rich dolomite, which is more labile, does not occur significantly in the Zar-3 storage site. This fact is very important for fluid–rock interactions modelling and will be discussed later. Calcite and dolomite (%) values calculated from TIC and clay minerals + quartz + feldspars content (Cl + Q + Fsp, Supplementary Table S4) for the reservoirs and caprocks are shown in a ternary diagram in Figure 7.

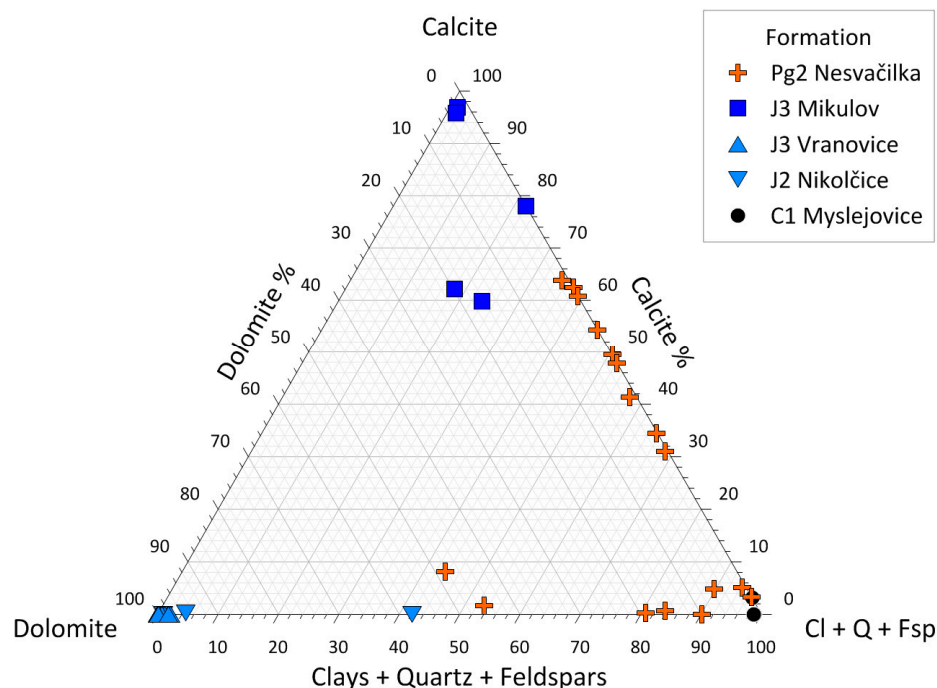


**Figure 7.** Ternary plot of dolomite, calcite, and clay mineral + quartz + feldspar content (Cl + Q + Fsp) in rock samples of the principal lithostratigraphic units of the Zar-3 storage complex listed in the legend; for more details, see Figure 4.

Vranovice Fm., the principal reservoir, represents an end-member lithology of almost pure dolomite (Figure 7). Nikolčice Fm., which underlies Vranovice Fm., is rich in dolomite but has also quartz and minor rock-building minerals, such as feldspars.

Overlying marls of the Mikulov Fm. form caprock 1, which shows a broad variety of mineral composition and contains little or no dolomite, abundant calcite and siliciclastics, mainly clay minerals and pyrite.

Caprock 2 is composed of Paleogene siltstones of the Nesvačilka Fm., which are rich in quartz, feldspars, clays and pyrite and have a variable amount of calcite. The mineral composition data were used, among others, for optimisation of the experimental conditions of the fluid–rock interactions dealt with in a follow-up paper.

### 6.3. Petrography

The reservoir and caprock characteristics were complemented by microscopy in translucent and fluorescent light. The carbonate petrographic descriptions and interpretations follow the principles outlined by [17] further developed by [18–20], rather than [21], even though the latter introduced many very bright ideas. The application of fluorescent microscopy profits from the experience shared by [22]. The reservoir samples are represented by Vranovice Fm. and Nikolčice Fm. rocks. Vranovice Fm. consists of dolostones with fine to coarse grain size, as well as rare oolitic limestones. Nikolčice Fm. is represented mainly by sandy dolostones with some quartz and feldspars.

Oolitic limestones (Figure 8) are present in the upper part of the Vranovice Fms. The rock can be characterised as oolitic packstone to grainstone with pellets. Micrite is partly recrystallised to dolomitic sparite or leached. Newly formed pyrite occurs in the samples. Ooide envelopes are developed in three types: (a) dark concentric, (b) micritic lacking texture and (c) light radial. Ooid centers are sometimes leached or recrystallised. Rarely, relics of fossils can be found in ooid centers. The facies can be assigned to a shelf lagoon with open circulation and moderate to low energy conditions. Limestone is affected by compaction and pressure dissolution resulting in the formation of stylolites. Oolitic limestones have orange fluorescence, most probably due to rich oil nano-inclusions.

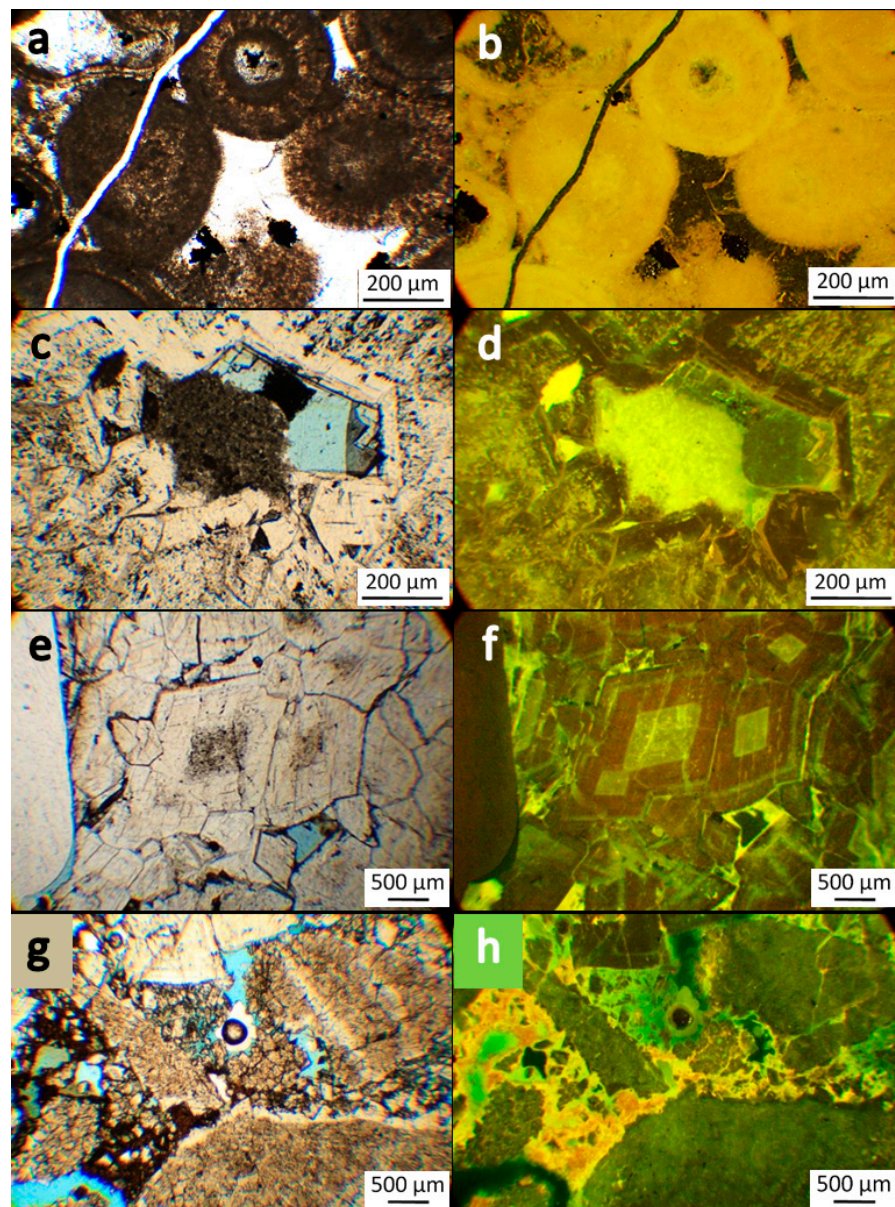


**Figure 8.** (a,b) Concentric and radial envelopes of ooides (Vranovice Fm. in PPL) showing orange fluorescence induced by bituminous nano-inclusions; (c,d) planar-s dolomite in Vranovice Fm. lining the pore partly filled by dolomicrite (PPL) has outer dark non fluorescent rim; (e,f) light dolomite crystals (PPL) show strong fluorescence zonation with dark dolomite rim and brighter core with micro-fluid inclusions; (g,h) heavily brecciated dolostone in the Vranovice Fm. cemented by fine grain dolomite and residual bitumens dark in PPL (g) and orange yellow in fluorescent light (h).

The majority of Vranovice Fm. consists of dolostones that have undergone multiple stages of dissolution (karstification), dolomitization and collapsing, resulting in brecciation and dolomite cementation. This can be demonstrated on medium-grained dolomite breccias, which are fully dolomitised and have collapsed rock texture. This process happened at very shallow marine conditions with periodical emerging and submerging below the sea level. The resulting highly vuggy porosity (cavernous and not interconnected) formed during the secondary stage of dolomite dissolution (Figure 8h). With increasing depth, the dolostone breccias tend to be more compacted and less porous. These observations confirm and complement the earlier studies of Jurassic carbonates in the SE Bohemian Massif [23].

Sandy calcareous or dolomitic siltstones of the Nesvačilka Fm. form seal 2. They overlie both the reservoir, Vranovice Fm., and seal 1, Mikulov Fm. (Figure 9a–d). Upper

sandstones are heterogeneous both in grain composition and size, ranging from tens of microns up to several mm. The minerals consist of quartz, feldspars, mica and clays accompanied by fossils and rare glauconite. The siltstones/sandstones have isopachous dolomite cement, which makes for poor communication among the intergranular pore systems. The lower part of the Nesvačilka Fm. is rather fine grained (below 200  $\mu\text{m}$ ; Figure 9c,d) and is built mainly by quartz and feldspars. The quartz grains are often cracked, while feldspars are degraded. The pore space is often filled by clay and silt and rarely by carbonate cement. Large detrital coal particles up to several cm in size were found in some of the Nesvačilka core samples.

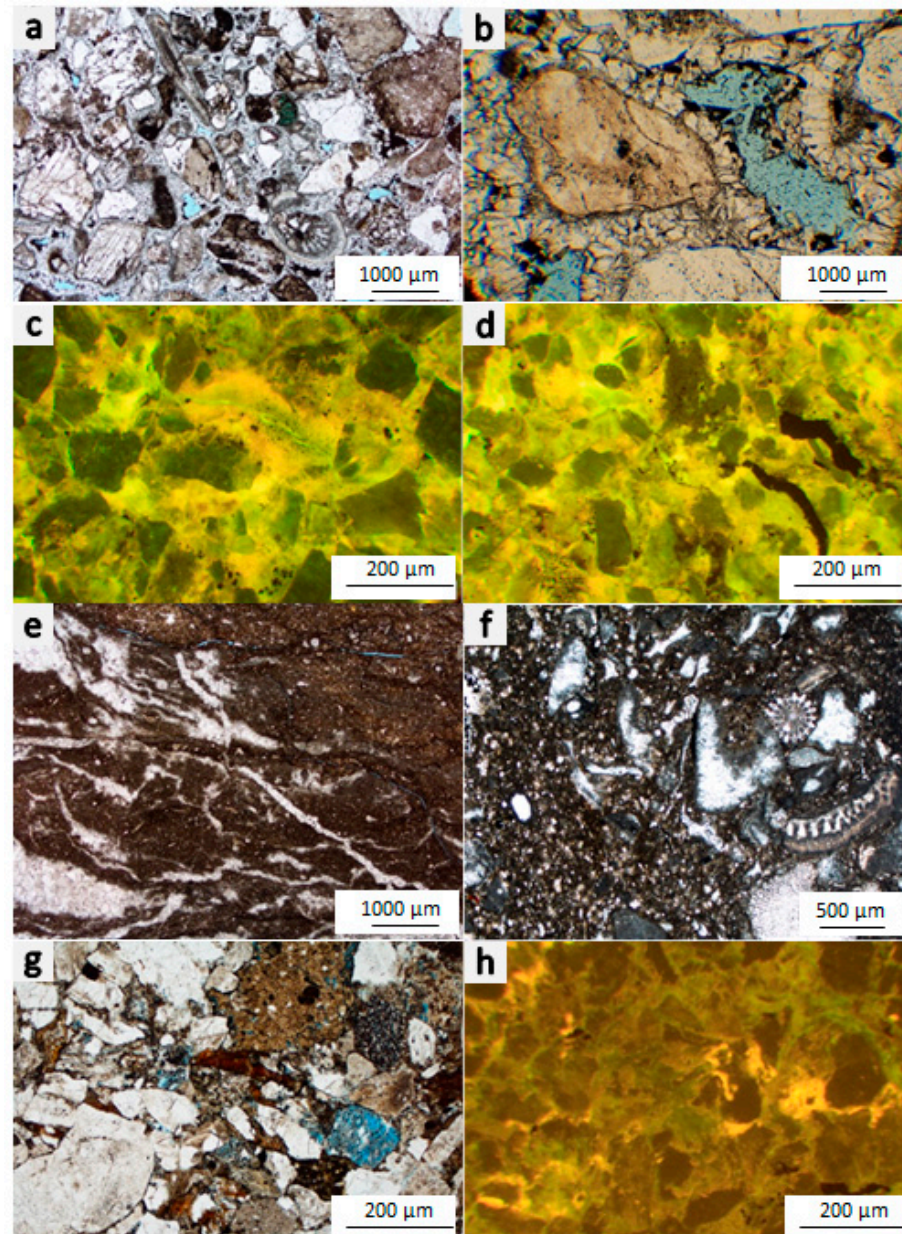


**Figure 9.** (a,b) Dolomitic sandy siltstone of the Nesvačilka Fm. is cemented by isopachous dolomite cement with remains of interparticle porosity; (c,d) sandy siltstone of the Nesvačilka Fm. with abundant bitumen impregnation marked by orange fluorescence; (e,f) fine grained marly wackestones of Mikulov Fm. rich in bioclasts; (g,h) silty sandstone of the Myslejovice Fm. with interparticle pores after feldspar dissolution filled by blue epoxy (g) and showing orange fluorescence of rarely occurring residual oil impregnations (h).

Seal 1, the Mikulov Fm., partly overlies the reservoir of the Vranovice Fm. from north and south (Figure 2). Petrologically, the Mikulov Fm. rocks range from marly wackestones (Figure 9e) to silty carbonatic sandstones (possibly equivalent to Falkenstein Fm. described in Austria). The rocks contain high amounts of clay, subangular bioclastic detritus and (sub)rounded intraclasts and pellets. The allochems are partly leached and recrystallised, forming minor moldic porosity (Figure 9f). The marls are composed of illite-smectite and chlorite-smectite clay and calcitic silt. The rocks exhibit mild fracture porosity and weaker dissolution features than the Vranovice Fm. Coarse-grained beds are rich in subangular quartz grains. The rock matrix is built by anhedral calcite crystals, possibly as a result of original micrite recrystallisation. Bituminous matter was scarcely recorded in fracture pores. Abundant kerogen type II of planktonic algal origin occurs as individual Prasinophyta alginite bodies and aggregated lamalginites. The latter are considered to be conduits of oil and gas migration from the deep-seated source rocks to carrier beds [9,13].

Stratified silty sandstones to arkoses of Carboniferous Myslejovice Fm. act as the bottom seal in the Zar-3 storage complex. The rocks are composed of subangular grains of quartz, feldspar and rare mica. The rocks are affected by compaction (fitted and sutured contacts of grains). The feldspars are intensely altered to clay minerals or dissolved (Figure 9g), forming modest interparticle porosity. Small compressed and elongated coal particles were observed in some of the sandstones. Fracture porosity is developed occasionally. Rare bituminous matter impregnations are observed in thin sections exhibiting orange fluorescence, indicating the thermal maturity of the oil window (Figure 9h).

#### 6.4. Optical and Hg Porosity

Reservoir and caprocks samples impregnated by blue epoxy resin were analysed for pore geometry using image analysis (Figure 10a–f). The relative area of open pores marked by blue colour with respect to the outlined total thin section area was evaluated as optical porosity following [24]. The interpreted pore size distributions suggest that in all rock types, the nano- and microporosity prevail (<10 µm). In the reservoir dolomites of the Vranovice Fm., dual cavernous and fracture macropores with diameters ranging from 100 to 300 µm contribute by 20–40% to the total porosity 2–8%<sub>abs</sub> (Figures 10 and 11) and may represent the effective porosity fraction available for fluid flow.

The caprocks have about 5–10 times lower porosity than the reservoir rocks and have the majority of pores in the clay size (<5 µm), which is considered to be the low-efficiency range for fluid migration because of the capillary forces.

The optical porosity data were compared with the mercury porosity (Figure 11). The optical porosity method has limitations in terms of neglecting too-big fractures, which usually do not permit the preparation of a representative thin section, not mentioning that the fractured cores, when brought to the surface, fall apart. The pores of <1 µm are difficult to impregnate and evaluate in visible-spectrum light. In spite of this fact, both methods concluded that the majority of the pores are in the micropore size range.

From the comparison in Figure 11, it follows that optical porosity shows details in the 20–30%<sub>rel</sub> macroporosity range, while 70–80%<sub>rel</sub> of the cumulative porosity remains at the micro-to-nano-scale and is optically difficult to quantify. For production purposes, the micro-nano-porosity was considered to be not efficient for active fluid flow. More research is needed on microscopic petrology and petrophysics on the same samples with respect to the behaviour of the minerals after exposure to the injected CO<sub>2</sub>.

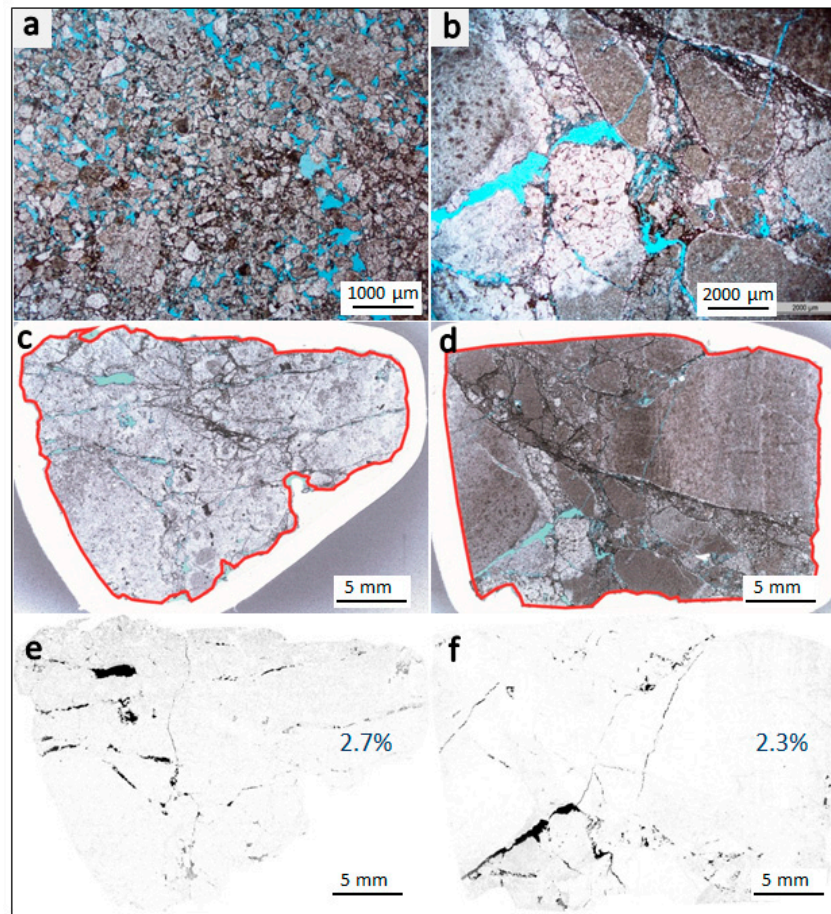


**Figure 10.** (a,b) Vranovice Fm. brecciated dolostones have undergone multiple processes, including dolomitisation, dissolution, karstification, collapses, brecciation and another stage of dissolution, forming fracture and vuggy porosity; (c,d) scanned whole thin section pictures of dolomite samples of the Vranovice Fm. Red line delineates the full evaluated area of the rock impregnated by blue epoxy resin; (e,f) separated blue pore areas represent fraction of 2.7 and 2.3% of the full area considered as optical porosity evaluated by image analysis. The pores shapes form vugs, fractures and pore (dis)connections.

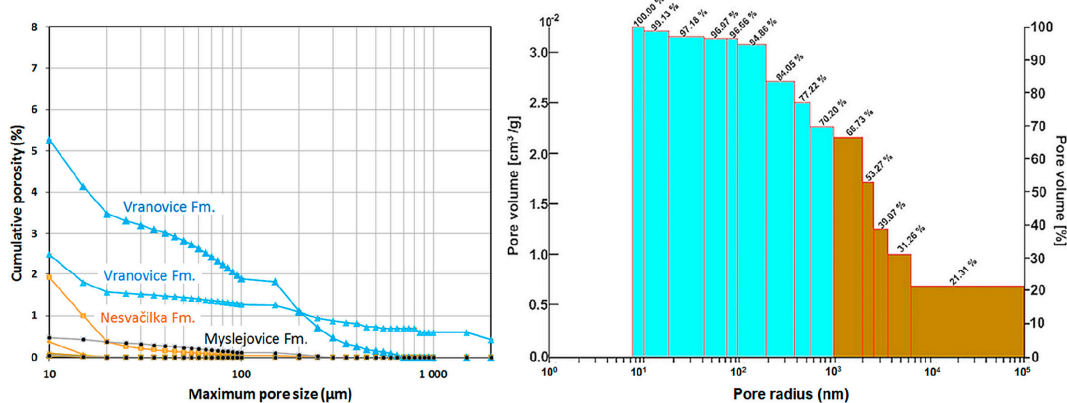


**Figure 11.** Distribution of cumulative optical porosity (left) as a function of pore size in reservoir rock (Vranovice Fm.: blue line) and caprocks (Myslejovice: black line and Nesvačilka Fms.: orange line). For comparison, mercury pore size distribution in the Vranovice Fm. reservoir is shown (right) with cumulative total porosity of 8%, which consists of macropores in brown and micropores in blue. The pore volume vertical axis is in relative % and 100%<sub>rel</sub> (right) = 8% total cumulative porosity (left).

### 6.5. Bitumens in Reservoir and Caprocks and Their Correlation with Reservoir Oils

The extractable organic matter in rocks (bitumen) was analysed for biomarkers by GC-MS. Selected parameters were evaluated evidencing the biological origin, depositional environment and thermal maturity [8,25,26]. The same parameters were analysed in all sedimentary formations and oils in the Zar-3 storage complex and broader vicinity. A mutual comparison was made of rocks and fluids and conclusions were drawn on fluid migration in the eastern Bohemian Massif below the West Carpathians.

The principal biomarker groups include triterpanes (hopanes), steranes and polycyclic aromatic hydrocarbons and their alkylated homologues (e.g., phenanthrenes). At shallow depths, the biomarker parameters mimic the biological configuration. With increasing depth and temperature, the molecules change to a more geological form [26]. The trend of the source rocks' thermal maturation is shown in Supplementary Table S5 and in Figure 12 with calculated vitrinite reflectance  $R_c$  based on the methylphenanthrene index MPI1 [27] measured in core samples from deep wells and oils in the broader Zar-3 neighbourhood incorporating the earlier data of [9]. Jurassic source rocks of the Mikulov Fm. show a very similar trend of thermal maturation to that of Paleogene Nesvačilka Fm., which was interpreted as evidence that there was no significant difference in the burial depth of the Jurassic and Paleogene in the geological past. The eroded Jurassic was substituted by the Paleogene and subsequent burial below the Outer Carpathian nappes played the key role in source rock maturation in the region [4]. In Figure 12, the oil samples are shown as green dots and their  $R_c$ -MPI1 values are higher than 0.8%. In other words, oil thermal maturity is equivalent to that of the source rocks at depth greater than 4–5 km from the surface. The oil produced from the ZA4a well has even higher thermal maturity ( $R_c$  of 1.0%). The reservoir rock extracts of the Zar-3 field show logically similar values to the oil (blue triangles). Interestingly, some of the Mikulov and Nesvačilka caprocks show more or less similar values to one another, probably due to the partial infiltration of the reservoir oil into the overlying seal.

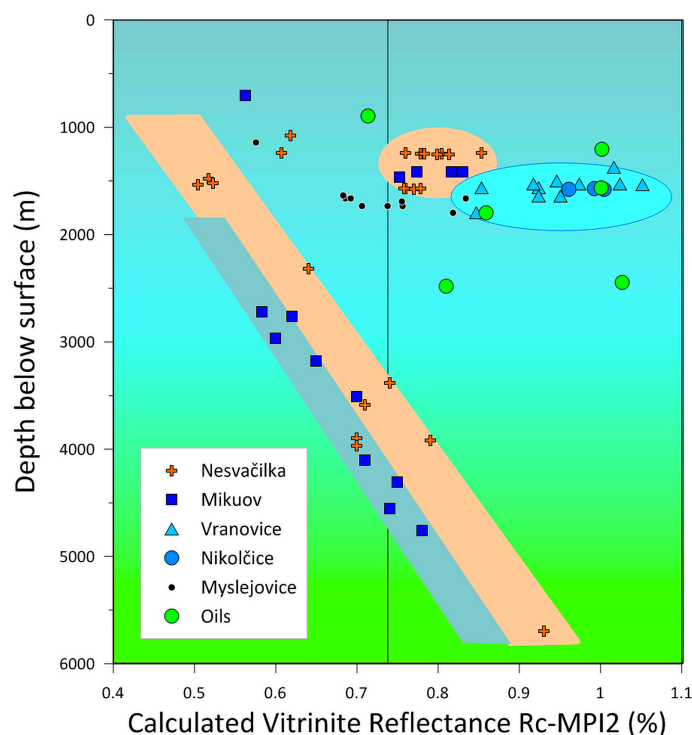


**Figure 12.** Calculated equivalent vitrinite reflectance ( $R_c$ -MPI1) based on methylphenanthrene index in Carboniferous (Myslejovice Fm.), Jurassic (Mikulov, Vranovice and Nikolčice Fms.) and Paleogene rocks (Nesvačilka Fm.) and oils from Zar-3 site and broader vicinity. Immature zone: blue, oil window: green.

The interpretation is that the oil and gas generation and the regional oil and gas migration in the eastern margin of the Bohemian Massif have occurred since the Middle Miocene, i.e., cca 16 Ma, as was also mentioned earlier by [4,9,28]. The migration took place at least 3–6 km vertically and 15–20 km horizontally below the West Carpathian fold-and-thrust belt. In this context, it is not surprising that the majority of the sedimentary formations of the Zar-3 storage complex were exposed to the migrating fluids and even to a slight impregnation of some seal horizons.

According to our interpretations, oil and gas accumulation formed in the dolomite reservoir of the Vranovice Fm. in the Zar-3 structure. The overlying Mikulov Fm. has acted up to now as an efficient caprock. Paleogene Nesvačilka Fm. is partly impregnated by bitumens genetically related the reservoir oil, but the impregnations formed by diffusive type of migration and are trapped in micropores, insofar that they act as caprock.

### 6.6. Oils

The Zar-3 oil samples are classified as medium sweet crude oils of 24° API gravity and viscosity of 40–50 mPa s. The whole oil analysis provided information on the gasoline and black oil fractions of oils (Figure 13). Most biomarkers occur in the black oil molecular fraction. The black oil is a residuum of the original oil accumulation affected by heavy biodegradation, which is classified as level 6 on the PM scale [25]. The thermal maturity data of oils are in the Supplementary Table S5 and in Figure 12.

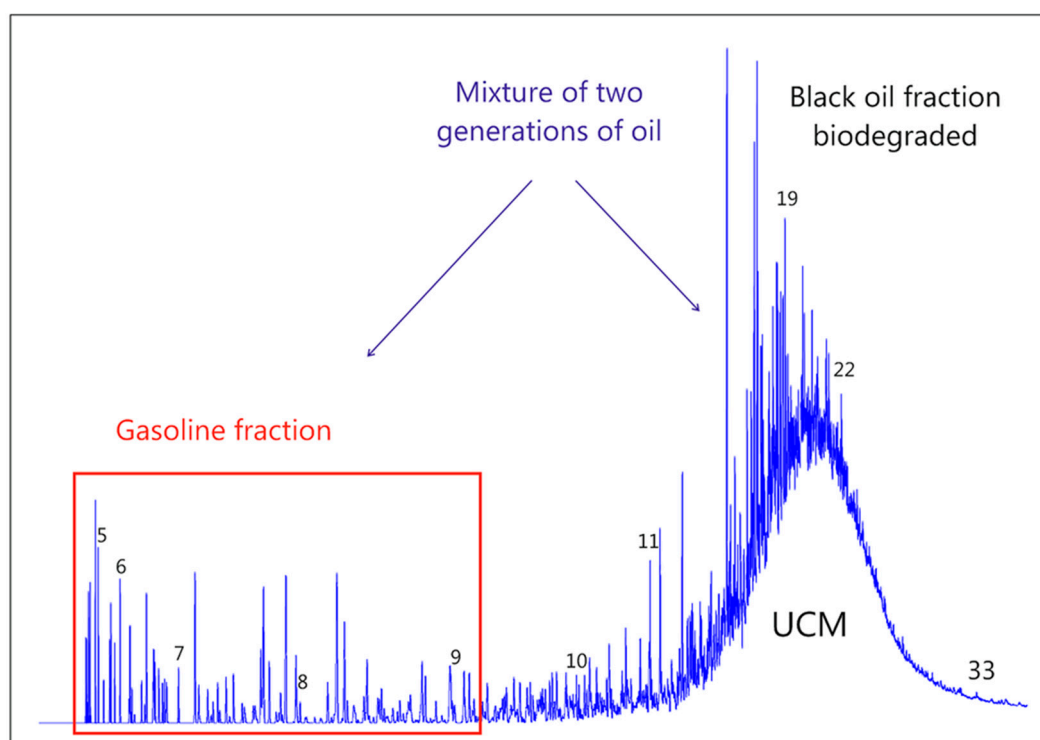


**Figure 13.** Whole oil gas chromatogram of the produced Zar-3 oil with detailed distribution of light hydrocarbons in the C<sub>5</sub>–C<sub>9</sub> range. Numbers show position of n-alkanes with the specified number of carbon atoms per molecule in the gasoline fraction and where they would occur if present in the black oil fraction.

The most striking feature in Figure 13 is the big UCM hump (unresolved compound mixture), which is a typical result of microbial biodegradation of oil at temperature below 65 °C. No or almost no n-alkanes are preserved in the C<sub>13</sub>–C<sub>35</sub> range. The majority of hydrocarbons in the gasoline fraction were quantified and the derived transformation and correlation ratios were calculated following [29–31]. The transformation in the reservoir shows different steps of biodegradation of the gasoline-range hydrocarbons from the

first “victims” removed from the mixture (n-C7) to those more resistant “leftovers” (e.g., dimethylcyclopentane). Additional alterations include water washing, which removes preferentially aromatic compounds, such as benzene, toluene and xylenes. Oils from Zar-3 and adjacent oil and gas fields were grouped based on the transformation ratios TR1–TR8 (Figure 14).

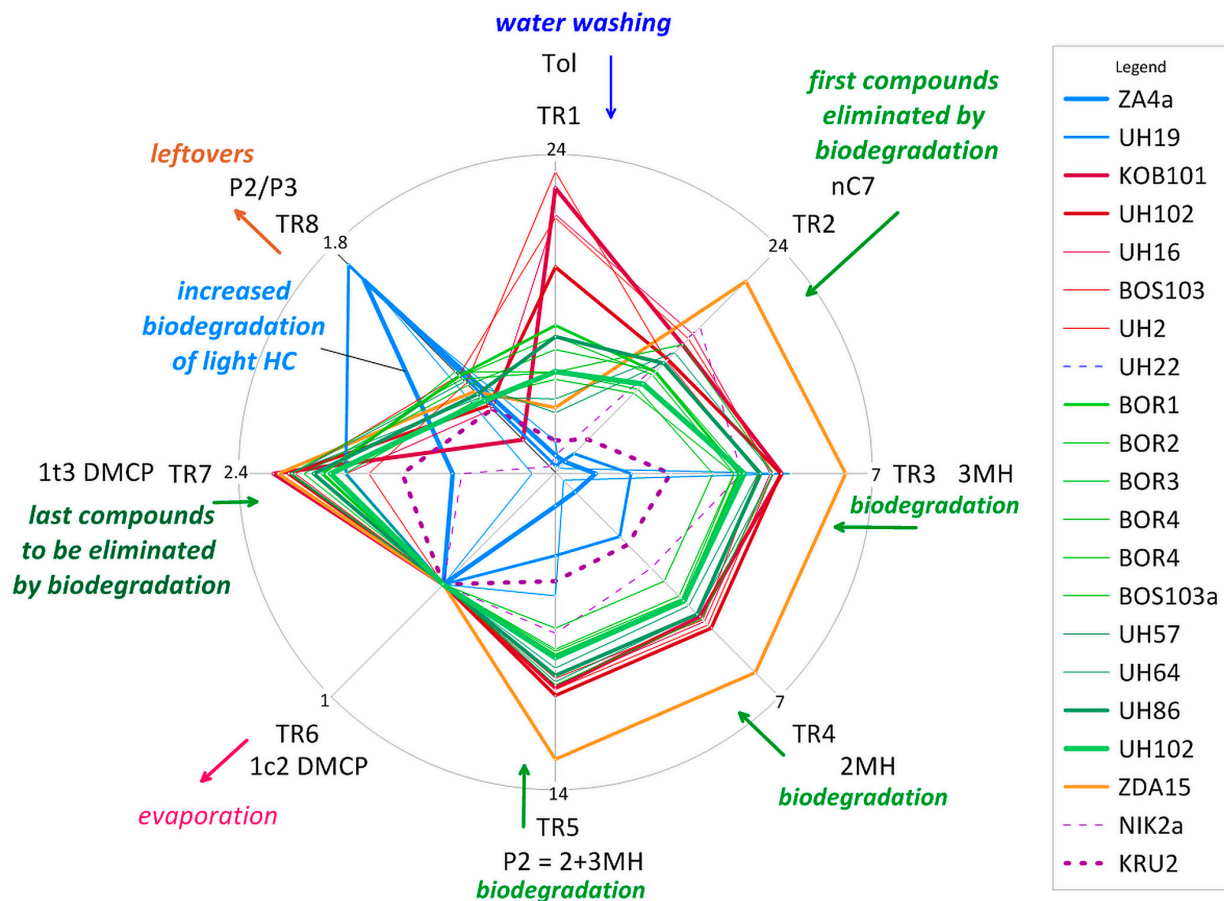


**Figure 14.** Transformation ratios of the Zar-3 oil and selected reference oil samples from the broader neighbourhood.

Our interpretation is that the first original accumulation formed after the oil generation and migration from Jurassic source rocks took place after the emplacement of the West Carpathians during the Lower-Middle Miocene (12–17 Ma). The accumulated oil underwent medium intensive biodegradation in the reservoir. Later, the biodegraded black oil mixed with gasoline-range light hydrocarbons (LHC), which arrived during a second migration event. In the Zar-3 reservoir, the LHC was biodegraded, but less so than the black oil, as the LHC still contains n-alkanes and iso- and cyclo-alkanes. The light hydrocarbons show higher thermal maturity and were generated from a greater burial depth and temperature of 125 °C using ratios of [30,31] than the black oil, as was observed earlier in a nearby Ždánice field [9,28].

### 6.7. Gases

Our interpretations of gas geochemistry are based on concepts outlined by [32–34]. The produced gas from the ZA4a well has 82–86% methane and 5.1–10.4% carbon dioxide. The carbon isotopic composition of methane  $\delta^{13}\text{C}(\text{CH}_4)$  of  $-37$  to  $-40\%$  (Supplementary Table S6 and Figure 15) suggests that methane is of purely thermogenic origin with no microbial gas contribution. The isotopic composition of carbon dioxide,  $\delta^{13}\text{C}(\text{CO}_2)$ , ranges from 6.9 to 16.2‰ and suggests that carbon dioxide originates from the dolomite dissolution. Traces of

H<sub>2</sub>S occurred at the annulus and may be associated with the reinjection of the formation water from the separator back to the aquifer.

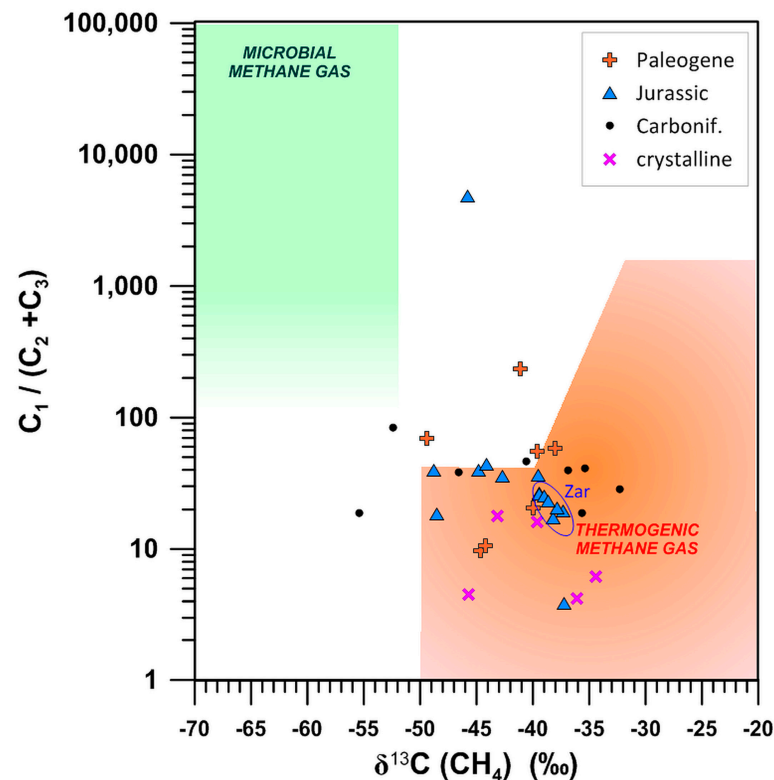


**Figure 15.** Zar-3 gas characteristics are shown in “Bernard” type plot based on  $\delta^{13}\text{C}(\text{CH}_4)$  carbon isotopic composition of methane and  $\text{C}_1/(\text{C}_2 + \text{C}_3)$ —dryness index from ZA3, ZA4a, ZA6, ZA8H, ZA14H and reference gas samples from the Uhřice, Dambořice (Jurassic and Carboniferous reservoirs) and Klobouky, Bošovice, Hostěradky, Násedlovice fields (Paleogene reservoirs). The interpretation fields of thermogenic and microbial gas origin are adapted from [32].

#### 6.8. Formation Water Mineralisation in the Reservoir, Overburden and Underlying Rocks

Formation water geochemical types from the Zar-3 storage site and adjacent oil and gas fields are shown in Figure 16 based on data in Supplementary Table S7. The mineralisation of the pore water is in general controlled by the original depositional environment and the secondary alterations due to fluid–rock interactions and infiltration of descending fresh water from the surface. The mineralisation expressed as the total dissolved solids in water (TDS) acquired from the CGS and MND databases covering the past 30 years is shown in Figure 17 with respect to depth in the broader Zar-3 area of interest. The following TDS ranges are observed in the overburden caprocks (15–22 g/L), main reservoirs (16–24 g/L) and underlying formations (20–33 g/L). The data suggest that the Zar-3 storage complex is a closed system. Fresh water infiltration into the overburden rocks evidenced by the TDS of <5 g/L are rarely observed and are limited to a depth of <1 km from the surface.

The current investigations provide the following update of the petroleum system evolution in the SE Bohemian Massif. The principal reservoir in the Zar-3 storage complex is a dolomite of the Vranovice Fm. with mainly fracture and minor vuggy porosity. Based on detailed petrography and geochemistry, the original limestone of the Vranovice Fm. formed most probably as a pinnacle reef, which periodically emerged from and submerged below the sea level. These conditions resulted in shallow-water dolomitisation. During emergence, karstification occurred, followed by collapses and brecciations. An additional reservoir, the Nikolčice Fm., occurs below the Vranovice Fm. It is built by quartz-dolomitic sandstone deposited in a shallower sea.

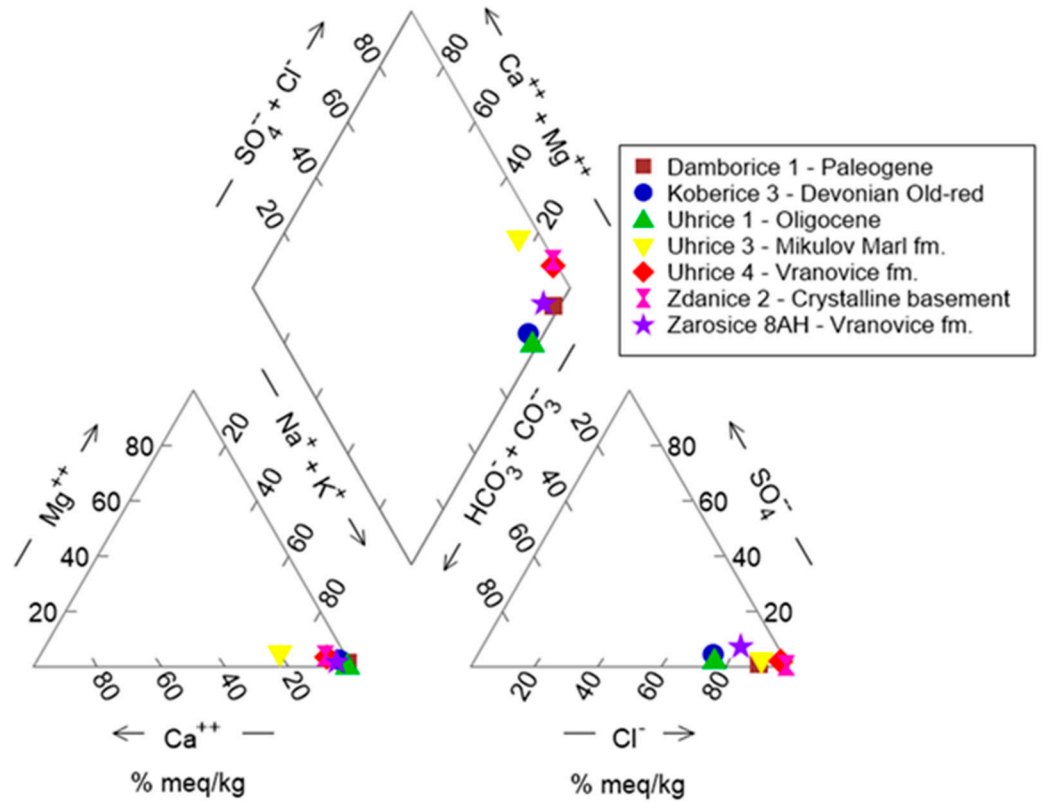


Figure 16. Piper plot of chemical composition of the formation water in the Žarošice and adjacent fields.

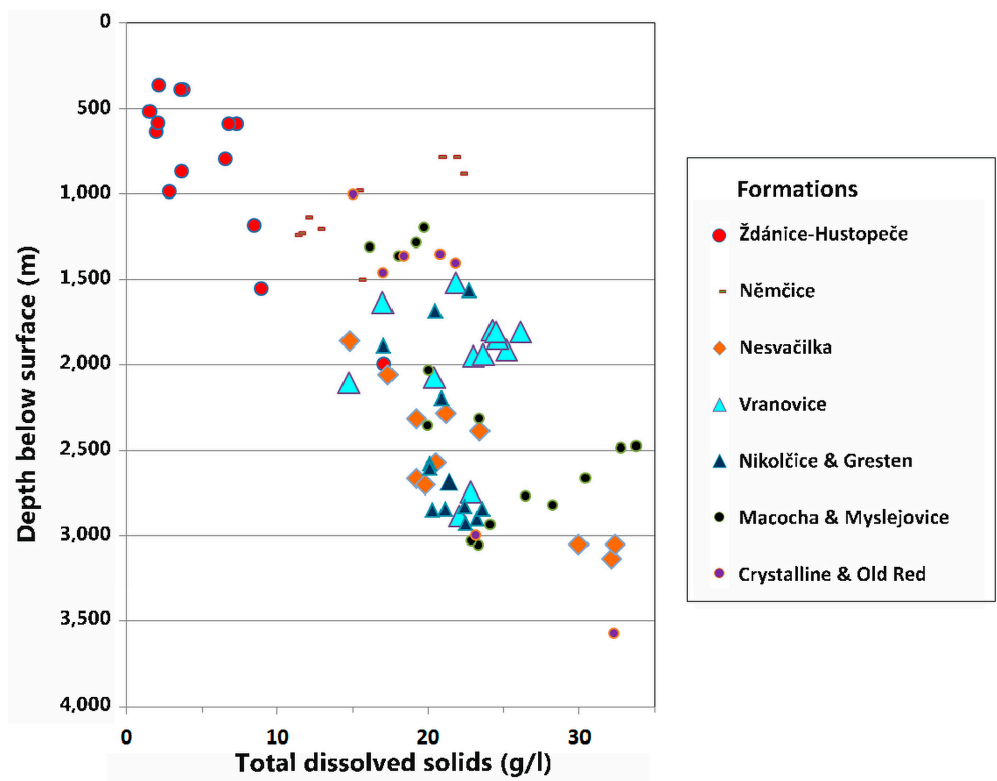


Figure 17. Mineralisation of formation water expressed as total dissolved solids in overburden, main reservoir and underlying strata of the broader region of Zar-3 storage site. Lithostratigraphic units in the legend include the reservoirs -Vranovice and Nikolčice Fms.; the rest mainly represent the seals, sometimes with limited porous intervals.

From the analysis of the reservoir–seal contact, it may be concluded that later, the reef with originally steep walls was drowned and at increased water depth marls of the Mikulov Fm. (here very similar to the Falkenstein Fm. described in Austria [4]) overlapped on the Vranovice Fm. Facial interfingering probably accompanied the deposition in the Oxfordian (Upper Jurassic). This caprock has very little or no dolomite; calcite is the major carbonate mineral constituent accompanied by clays and some quartz.

During the Cretaceous and Lower Paleogene, deep submarine canyons were incised into Jurassic formations and even steeper walls of the earlier reef of the Vranovice Fm. were created by stream erosion. Part of the Mikulov Fm. (caprock) was also removed in the western part of the Zar-3 structure.

In the Eocene, sandy and shaly siltstones of the Těšany (not present in the Zar-3) and Nesvačilka Fms. (present in Zar-3) were deposited in the canyons often bordered by steep walls of the Jurassic. These rocks have variable carbonate cement content and are enriched in sulphur minerals.

In the Early-to-Middle Miocene, the West Carpathian units were thrust on and buried the eastern margin of the Bohemian Massif to depth. As a result, Jurassic source rocks were exposed to an increased temperature and oil and gas generation took place. The oil window is documented here and was mentioned by [9] to occur at a depth of 4–6 km, with gas generation at 6–9 km.

Since that time, regional migration of oil and gas occurred and all the formations in Zar-3 storage site were exposed to hydrocarbon migration. A 105 m thick oil column and additional 150 m of gas cap accumulated in the Zar-3 reservoir of the Vranovice and Nikolčice Fms [3]. This provides strong evidence that the Zar-3 structure was efficiently sealed.

## 7. Conclusions

The reservoir dolomite of the Vranovice Fm. in the Zar-3 storage complex has dual porosity with prevailing fracture and minor vuggy (cavernous) porosity. Shallow dolomitisation, karstification, collapses and brecciations resulted in random fracture orientation. The contact of seal 1 (Mikulov Fm.) and the reservoir of the Vranovice Fm. is an onlap. Significant erosion is observed at the contact of seal 2 (Nesvačilka Fm.) and the reservoir. Seal 3 (the Ždánice overthrust unit with the Němčice Fm.) is superimposed on both seal 1 and 2.

All three caprocks show 5–10 (or more) times lower optical porosity than the reservoir rocks. Micro-nanoporosity is dominant in all caprocks. Bitumen (oily) impregnations are observed everywhere in the reservoir and partly also in the Nesvačilka Fm. based on MudLogs, fluorescent microscopy and biomarkers. Both in Mikulov Fm. and in the Ždánice overthrust unit, the bitumen impregnations are very rare or absent.

The oil in the Zar-3 reservoir consists of gasoline-range hydrocarbons mixed with black oil. They are of different depth of origin and migration phase. The black oil fraction of the Zar-3 oil is heavily biodegraded in the reservoir. All n-alkanes were removed by bacteria. The present UCM (unresolved compound mixture) represents cca 78% of the oil. This feature is typical of a higher biodegradation level (PM6). The thermal maturity of the black oil fraction is equivalent to a vitrinite reflectance of 0.86%, which occurs in Jurassic source rocks at a depth of ca 5 km. Light hydrocarbons (gasoline fraction) are of higher thermal maturity, equivalent to a temperature of 125 °C, and migrated during a later phase of migration, probably in the Upper Miocene. The gasoline fraction is mildly biodegraded in the reservoir, and the n-alkanes are at least partly preserved. Gasoline-range hydrocarbons in Zar-3 show a very high water washing effect evidenced by the loss of the aromatic hydrocarbons and a higher biodegradation level than the gasolines in the adjacent oil fields. Four to five genetic groups were identified among the gasoline fraction of the oils in the region. ZA4A oil is most similar to the nearby UH57, UH19 and NIK2A.

Gas in the Zar-3 has in average 82–86% methane and 5.1–10.4% carbon dioxide. The carbon isotopic composition  $\delta^{13}\text{C}(\text{CH}_4)$  of  $-37$  to  $-40\text{‰}$  suggests that the methane is of purely thermogenic origin with no microbial contribution. The carbon isotopic com-

position of carbon dioxide— $\delta^{13}\text{C}(\text{CO}_2)$  ranges from 6.9 to 16.2‰ and suggests that the carbon dioxide originates from dolomite dissolution. Hydrogen sulphide occurs at the annulus irregularly up to 10 mg/m<sup>3</sup> gas. In the produced gas, it was found to be mostly <2 mg/m<sup>3</sup> gas.

The formation water in the Zar-3 reservoir is of Na-Cl type with a mineralisation (TDS) of 24–26 g/L. The formation water mineralisation parameter (TDS) is the highest in the underlying Devonian and Carboniferous units and in the weathered crystalline basement. The overburden caprock formations have water with decreasing upward mineralisation, still similar to that of the main reservoir. The infiltration of fresh water is not observed at depths > 1 km from the surface.

It may be concluded that all the caprocks sealed the reservoir at a sufficient level to accumulate a ca. 105 m high original oil column and a ca. 150 m gas cap column and that it will efficiently seal the future CO<sub>2</sub> storage complex.

**Supplementary Materials:** The following supporting information can be downloaded at: <https://www.mdpi.com/article/10.3390/geosciences14050119/s1>, Geochemical data: Table S1. Elemental analysis of the cuttings samples from the ZA3 well. Table S2. Elemental analysis of core samples from selected wells in the broader Zar-3 area. Table S3. Rock-Eval 6 pyrolysis data of the ZA3 drilling cuttings. Table S4. Mineralogical composition of the core samples from wells in broader Zar-3 area. Table S5. Thermal maturity of rocks and oils based on Methylphenanthrene index MPI1. Table S6. Gas geochemistry—chemical and isotopic composition of carbon and hydrogen. Table S7. Formation water chemistry in deep wells in Zar-3 storage site and broader neighborhood.

**Author Contributions:** Conceptualisation, J.F. and M.P.; methodology, D.O., P.P., J.V. and M.L.; validation, M.P., D.O., P.P. and J.V.; writing—original draft preparation, J.F., D.O., P.P., M.P., J.V., V.O., M.L. and P.J.; writing—review and editing, J.F., M.P. and P.J.; visualisation, J.F., J.V. and M.P.; supervision, J.F.; project administration, J.F. All authors have read and agreed to the published version of the manuscript.

**Funding:** This research was funded by EEA—Norway Grants and Technology Agency of the Czech Republic (TA ČR) within the CO<sub>2</sub>-SPICER project (No: TO01000112, CO<sub>2</sub> Storage Pilot in a CarbonatE Reservoir).

**Data Availability Statement:** All data in Supplemental Files are open to all without requesting permission to download.

**Acknowledgments:** Core and cuttings samples and archival data were kindly provided by the MND a.s. company. The academic license of Schlumberger–Petrel and Petromod v 2021 software for students involved in the project is very much appreciated. Š. Káňa, B. Janíková and F. Buzek are very much acknowledged for their valuable assistance with the analyses and text preparation. The final manuscript benefited greatly from the criticism and suggestions by three reviewers. More information about the project can be found at [co2-spicer.geology.cz](http://co2-spicer.geology.cz).

**Conflicts of Interest:** The authors declare no conflicts of interest. The funders had no role in the design of the study; in the collection, analyses or interpretation of data; in the writing of the manuscript; or in the decision to publish the results.

## Abbreviations

API gravity	American Petroleum Institute oil gravity
ARO	aromatic fraction
C1	Lower Carboniferous
CaCO <sub>3</sub>	calcium carbonate
CEC	total cation exchange capacity
Cl + Q + Fsp	clay minerals + quartz + feldspars content
CO <sub>2</sub>	carbon dioxide
DCM	dichloromethane
Fm.	formation (lithostratigraphic unit)
GC-MS	gas chromatography-mass spectrometry

HCl	hydrochloric acid
HI	hydrogen index of Rock-Eval analysis $HI = 100 \times S2/TOC$ (mg/g TOC)
J3	Upper Jurassic
LHC	light hydrocarbons (C5–C9)
Ma	million years before present
Mb.	member (lithostratigraphic unit)
MPI	methylphenanthrene index
NPL	non-polarised light
NSO	polar fraction
OI	oxygen index of Rock-Eval analysis $OI = 100 \times S3/TOC$ (mg/g TOC)
Pg2	Middle Paleogene
PPL	plane-polarised light
Rc	calculated vitrinite reflectance
Rc-MPI1	calculated equivalent vitrinite reflectance based on methylphenanthrene index 1
S1	free hydrocarbons of Rock-Eval analysis (mg/g rock)
S2	pyrolytic hydrocarbons of Rock-Eval analysis (mg/g rock)
S3	pyrolytic CO <sub>2</sub> released by Rock-Eval analysis (mg/g rock)
SAT	saturated fraction
SRB	sulphate-reducing bacteria
TDS	total dissolved solids (mg/L)
TIC	total inorganic carbon (% <sub>m</sub> )
Tmax	temperature at maximum of S2 peak of Rock-Eval analysis (°C)
TOC	total organic carbon (% <sub>m</sub> )
TR	transformation ratio $TR = S1/(S1 + S2)$
TS	total sulphur (% <sub>m</sub> )
TVDSS	true vertical depth sub-sea (m)
UCM	unresolved compound mixture
UV	ultra-violet light
VPDB	Vienna-Pee Dee Belemnite standard used for $\delta^{13}C$ notation
VSMOW	Vienna-Standard Mean Ocean Water used for $\delta^2H$ notation
XPL	cross-polarised light
XRD	X-ray diffraction
XRF	X-ray fluorescence

## References

- Krejci, O.; Francu, J.; Poelchau, H.S.; Müller, P.; Stranik, Z. Tectonic evolution and oil and gas generation model in the contact area of the North European Platform with the West Carpathians. In *Oil and Gas in Alpidic Thrustbelts and Basins of Central and Eastern Europe*; Wessely, G., Liebl, W., Eds.; EAPG Spec. Publ. No. 5; Geological Society Publishing House: Bath, UK, 1996; pp. 177–186. [\[CrossRef\]](#)
- Adámek, J. The Jurassic floor of the Bohemian Massif in Moravia—Geology and paleogeography. *Bull. Geosci.* **2005**, *80*, 291–305.
- Kostelníček, P.; Ciprys, V.; Berka, J. Examples of Recently Discovered Oil and Gas Fields in the Carpathian Foredeep and in the European Foreland Plate underneath the Carpathian Thrust Belt, Czech Republic. In *The Carpathians and Their Foreland: Geology and Hydrocarbon Resources*; Golonka, J., Picha, F.J., Eds.; AAPG Memoir: Tulsa, OK, USA, 2006; Volume 84, pp. 177–190. [\[CrossRef\]](#)
- Picha, F.J.; Stranik, Z.; Krejci, O. Geology and hydrocarbon resources of the Outer Western Carpathians and their foreland, Czech Republic. In *The Carpathians and Their Foreland: Geology and Hydrocarbon Resources*; Golonka, J., Picha, F.J., Eds.; AAPG Memoir: Tulsa, OK, USA, 2006; Volume 84, pp. 49–175. [\[CrossRef\]](#)
- Tissot, B.; Welte, D.H. *Petroleum Formation and Occurrence*; Springer: Berlin/Heidelberg, Germany; New York, NY, USA; Tokyo, Japan, 1984; 699p. [\[CrossRef\]](#)
- Hunt, J.M. *Petroleum Geochemistry and Geology*, 2nd ed.; Freeman: New York, NY, USA, 1996; 743p.
- Lafargue, E.; Espitalié, J.; Marquis, F.; Pillot, D. Rock-Eval 6 applications in hydrocarbon exploration, production and in soil contamination. *Rev. L'institut Franc. Pétrole* **1998**, *53*, 421–437. [\[CrossRef\]](#)
- Dembicki, H. *Practical Petroleum Geochemistry for Exploration and Production*; Elsevier: Amsterdam, The Netherlands; Boston, MA, USA; Heidelberg, Germany; London, UK, 2017; 331p. [\[CrossRef\]](#)
- Francu, J.; Radke, M.; Schaefer, R.G.; Poelchau, H.S.; Caslavsky, J.; Bohacek, Z. Oil-oil and oil-source rock correlation in the northern Vienna basin and adjacent Flysch Zone. In *Oil and Gas in Alpidic Thrustbelts and Basins of Central and Eastern Europe*; Wessely, G., Liebl, W., Eds.; EAPG Spec. Publ. No. 5; Geological Society Publishing House: Bath, UK, 1996; pp. 343–354. [\[CrossRef\]](#)

10. Jirman, P.; Geršlová, E.; Bubík, M.; Sachsenhofer, R.F.; Bechtel, A.; Wieclaw, D. Depositional environment and hydrocarbon potential of the Oligocene Menilite Formation in the Western Carpathians: A case study from the Loučka section (Czech Republic). *Mar. Pet. Geol.* **2019**, *107*, 334–350. [CrossRef]
11. Jirman, P.; Geršlová, E.; Pupp, M.; Bubík, M. Geochemical characteristics, thermal maturity and source rock potential of the Oligocene Šitbořice Member of the Menilite Formation in the Ždánice Unit (Czech Republic). *Geol. Q.* **2018**, *62*, 858–872. [CrossRef]
12. Sachsenhofer, R.F.; Popov, S.V.; Bechtel, A.; Coric, S.; Francu, J.; Gratzer, R.; Grunert, P.; Kotarba, M.; Mayer, J.; Pupp, M.; et al. Oligocene and Lower Miocene source rocks in the Paratethys: Palaeogeographic and stratigraphic controls. In *Petroleum Geology of the Black Sea*; Simmons, M.D., Tari, G.C., Okay, A.I., Eds.; Geological Society; Special Publications: London, UK, 2018; Volume 464, pp. 267–306. [CrossRef]
13. Francu, J.; Horsfield, B.; Schenk, H.J. Jurassic source rock kinetics and the petroleum system of the SE Bohemian Massif. In *Book of Abstracts, 26th International Meeting on Organic Geochemistry*; González-Pérez, J.A., González-Vila, F.J., Jiménez-Morillo, N.T., Almendros, G., Eds.; Digital.CSIC, the Institutional Repository of “Consejo Superior de Investigaciones Científicas” (CSIC): Tenerife, Spain, 2013; Volume 2, pp. 391–392.
14. Geršlová, E.; Opletal, V.; Sýkorová, I.; Sedláková, I.; Geršl, M. A geochemical and petrographical characterization of organic matter in the Jurassic Mikulov Marls from the Czech Republic. *Int. J. Coal Geol.* **2015**, *141–142*, 42–50. [CrossRef]
15. Francu, E.; Francu, J.; Kalvoda, J.; Poelchau, H.S.; Otava, J. Burial and uplift history of the Palaeozoic Flysch in the Variscan foreland basin (SE Bohemian Massif, Czech Republic). In *Continental Collision and the Tectono-Sedimentary Evolution of Forelands: European Geosciences Union-Stephan Mueller Special Publication Series*; Bertotti, G., Schulmann, K., Cloetingh, S., Eds.; European Geosciences Union: Munich, Germany, 2002; Volume 1, pp. 167–179. [CrossRef]
16. Ladwein, H.W. Organic geochemistry of Vienna Basin: Model for hydrocarbon generation in overthrust belts. *AAPG Bull.* **1988**, *72*, 586–599. [CrossRef]
17. Dunham, R.J. Classification of carbonate rocks according to depositional texture. In *Classification of Carbonate Rocks*; Ham, W.E., Ed.; AAPG Mem: Houston, TX, USA, 1962; Volume 1, pp. 108–121. [CrossRef]
18. Embry, A.F.; Klovan, J.E. A late Devonian reef tract on northeastern Banks Island, N.W.T. *Bull. Can. Pet. Geol.* **1971**, *19*, 730–781. [CrossRef]
19. Lokier, S.W.; Al Junaibi, M. The petrographic description of carbonate facies: Are we all speaking the same language? *Sedimentology* **2016**, *63*, 1843–1885. [CrossRef]
20. Wright, V.P. A revised Classification of Limestones. *Sediment. Geol.* **1992**, *76*, 177–185. [CrossRef]
21. Folk, R.L. Practical petrographic classification of limestones. *AAPG Bull.* **1959**, *43*, 1–38. [CrossRef]
22. Dravis, J.J.; Yurewicz, D. Enhanced carbonate petrography using fluorescence microscopy. *J. Sediment. Petrol.* **1985**, *55*, 795–804. [CrossRef]
23. Jurenka, L.; Francu, J. Application of fluorescent light microscopy to enhanced microfacies analysis of Jurassic carbonate rocks, SE Bohemian Massif. *Geol. Res. Morav. Sil.* **2020**, *27*, 106–110. [CrossRef]
24. Grove, C.; Jerram, D.A. jPOR: An ImageJ macro to quantify total optical porosity from blue-stained thin sections. *Comput. Geosci.* **2011**, *37*, 1850–1859. [CrossRef]
25. Weiss, H.M.; Wilhelms, A.; Mills, N.; Scotchmer, J.; Hall, P.B.; Lind, K.; Brekke, T. NIGOGA—The Norwegian Industry Guide to Organic Geochemical Analyses [Online]. Edition 4.0 Published by Norsk Hydro, Statoil, Geolab Nor, SINTEF Petroleum Research and the Norwegian Petroleum Directorate. 2000, p. 102. Available online: <http://www.npd.no/engelsk/nigoga/default.htm> (accessed on 17 July 2000).
26. Peters, K.E.; Walters, C.C.; Moldowan, J.M. *The Biomarker Guide: Part I, Biomarkers and Isotopes in the Environment and Human History; Part II, Biomarkers and Isotopes in Petroleum Systems and Earth History*, 2nd ed.; Cambridge University Press: Cambridge, UK, 2005; 1155p. [CrossRef]
27. Radke, M.; Welte, D.H.; Willsch, H. Geochemical study on a well in the Western Canada Basin: Relation of the aromatic distribution pattern to maturity of organic matter. *Geochim. Cosmochim. Acta* **1982**, *46*, 1–10. [CrossRef]
28. Picha, F.J.; Peters, K.E. Biomarker oil-to-source rock correlation in the Western Carpathians and their foreland, Czech Republic. *Pet. Geosci.* **1998**, *4*, 289–302. [CrossRef]
29. Halpern, H.I. Development and applications of light hydrocarbon-based star diagrams. *AAPG Bull.* **1995**, *79*, 801–815. [CrossRef]
30. Mango, F.D. The light hydrocarbons in petroleum: A critical review. *Org. Geochem.* **1997**, *26*, 417–440. [CrossRef]
31. Thompson, K.F.M. Gas-condensate migration and oil fractionation in deltaic systems. *Mar. Pet. Geol.* **1988**, *5*, 237–246. [CrossRef]
32. Whiticar, M.J. Carbon and hydrogen isotope systematics of bacterial formation and oxidation of methane. *Chem. Geol.* **1999**, *161*, 291–314. [CrossRef]
33. Whiticar, M.J.; Faber, E.; Schoell, M. Biogenic methane formation in marine and freshwater environments: CO<sub>2</sub> reduction vs. acetate fermentation—Isotope evidence. *Geochim. Cosmochim. Acta* **1986**, *50*, 693–709. [CrossRef]
34. Milkov, A.V.; Etiope, G. Revised genetic diagrams for natural gases based on a global dataset of >20,000 samples. *Org. Geochem.* **2018**, *125*, 109–120. [CrossRef]

**Disclaimer/Publisher’s Note:** The statements, opinions and data contained in all publications are solely those of the individual author(s) and contributor(s) and not of MDPI and/or the editor(s). MDPI and/or the editor(s) disclaim responsibility for any injury to people or property resulting from any ideas, methods, instructions or products referred to in the content.